

Visualization and Planning of Neurosurgical Interventions with Straight Access

Nikhil V. Navkar¹, Nikolaos V. Tsekos^{*1}, Jason R. Stafford²,
Jeffrey S. Weinberg², and Zhigang Deng^{*1}

¹ University of Houston, Department of Computer Science, Houston, TX

² University of Texas, MD Anderson Cancer Center, Houston, TX

Contacts*: {ntsekos|zdeng}@cs.uh.edu

Abstract. Image-guided neurosurgical interventional procedures utilize medical imaging techniques to identify the most appropriate path for accessing a targeted structure. Often, preoperative planning entails the use of multi-contrast or multi-modal imaging for assessing different aspects of patient’s pathophysiology related to the procedure. Comprehensive visualization and manipulation of such large volume of three-dimensional anatomical information is a major challenge. In this work we propose a technique for simple and efficient visualization of the region of intervention for neurosurgical procedures. It is done through the generation of access maps on the surface of the patient’s skin, which assists a neurosurgeon in selecting the most appropriate path of access by avoiding vital structures and minimizing potential trauma to healthy tissue. Our preliminary evaluation showed that this technique is effective as well as easy to use for planning neurosurgical interventions such as biopsies, deep brain stimulation, ablation of brain lesions.

1 Introduction

Currently, we witness the rapid evolution of minimally invasive surgeries and image guided interventions that can lead to improved and cost effective patient treatments. It is becoming apparent that sustaining and expanding this paradigm shift would require new computational methodology that could assist surgeons in planning these procedures. A major challenge at either the preoperative or the intraoperative stage of an image guided procedure is visualization, comprehension and manipulation of a large volume of three-dimensional (3D) anatomical data.

Most often, 3D models of the brain tissue are generated after segmentation and rendering of the different anatomies. The operator may use those models for manual or computer-assisted selection of appropriate paths to access the targeted anatomy/structure. When a straight tool such as a biopsy needle or an applicator is used, the interventional task maybe approached as a two-point access practice, i.e. the point representing the entrance and the target. Since the target location is well known from the original inspection of images, it would be helpful to visualize the outer surface of the patient by incorporating information

about the underlying tissue. In this work we present a preliminary technique to such a visualization allowing for quantitative or semi-quantitative comparison among various points of entrance for neurosurgical procedures that require straight access. The main contribution of our work is the generation of access maps on the surface of patient's head which provide a neurosurgeon with plethora of meaningful information about the anatomy of the region of intervention and safety of selected insertion paths. In addition, our preliminary evaluation results showed that our method was intuitive and easy to use for neurosurgeons, which makes our technique clinically applicable. Meanwhile, the approach can be used in conjunction with existing visualization techniques to further improve the preoperative planning process.

A large volume of work in the field of neurosurgical planning is primarily focused on the development of computational methods to process and visualize multi-modality 3D data sets and generate 3D models of the brain (e.g. [10, 13, 11, 12]). The models are generated by using either multi volumetric or iso-surface rendering methods. Although, these approaches have been proved efficient in generating realistic and highly accurate 3D representations of the anatomy of the brain, they do not provide the extra quantitative information (apart from visualization) which would help neurosurgeons in making decisions during pre-operative planning.

For neurosurgical interventions, many studies have introduced approaches for path planning [7, 9, 5, 8, 6]. Lee et al. [7] and Nowinsky et al. [5] have incorporated the use of brain atlases for improving stereotactic neurosurgery. Although such an approach may allow for high fidelity tissue classification, it requires manual selection of the entry points. Bourbakis et al. [8] proposed another approach for 3D visualization pertinent to image guided brain surgery based on replicating surgeon behavior and decision-making. This approach requires user input to set appropriate parameters for calculating insertion points. Fujii et al. [9] proposed an automatic neurosurgical path-searching algorithm that requires assigning importance values to the cutting and touching of different tissues based on anatomical knowledge and the experience of neurosurgeons, which might not be very intuitive. This approach also incorporates blood vessels into the path searching algorithm by assigning them a cost value. For this part, it extracts a centerline for the vessels and then assumes a cylindrical shape that may not be close to the real anatomy. The algorithm finds a curvilinear path, which is not suited for straight-access interventions by current interventional tools. Most closely related to our work is that of Brunenberg et al. [6] which automatically calculates the possible trajectories for implantation of electrodes to selected targets for deep brain stimulation. This algorithm calculates safe paths automatically without significant user input. However, it requires segmenting the insertion path at regular intervals. The distance from each point at given regular intervals to every point on the vessels needs to be calculated. This is time consuming. In our work, we use a mesh-based representation of the anatomical structures that does not require segmenting the path; the minimum distance of the path to any point on the vessel is then directly computed and visualized.

2 Materials and Methods

2.1 Generation of Access Maps

In a generalized approach, the performance of a minimally invasive intervention with a straight tubular tool can be viewed as defining two points in a 3D space: the point of insertion of the tool and the targeted structure. Those two points define a path of insertion. Tomographic modalities, such as MRI or CT, offer 3D imaging thereby providing the means of such stereotactic approach. Since the target is a well-defined point in space (selected by inspecting the images), the problem of path planning is to select an entry point on the skin of the patient's head. We hypothesize that, by projecting the underlying brain tissue on the skin, it is possible to have a simple and intuitive selection of access paths. Since the preparatory stage of our approach (as discussed in section 2.2) renders anatomical structures with a mesh, without the loss of generality, the task of path planning is to find a vertex which is most suitable for incision. We assume that $\mathbf{M}_s = (\mathbf{V}_s, \mathbf{F}_s)$ is a mesh that corresponds to the reconstructed skin on patient's head with vertices \mathbf{V}_s and faces \mathbf{F}_s . The insertion vertex \mathbf{v} , where $\mathbf{v} \in \mathbf{V}_s$, is selected such that a line drawn from this vertex to a target point \mathbf{t} , where $\mathbf{t} \in \mathbf{R}^3$, defines a safe insertion path. In our approach, to achieve a high efficiency in the manual portion of planning, i.e. when the point of entrance is selected by the neurosurgeon, all the computationally intensive parts will be performed during the preparatory phase. Every vertex in the mesh \mathbf{M}_s corresponds to a possible incision point on the surface of the patient's head.

In order to find a set of vertices $\mathbf{V}_{\text{safe}} \subset \mathbf{V}_s$ that corresponds to safe incision points, our approach entails the generation of three access maps on the surface of the patient's head that can be used by the neurosurgeon to select an optimal path of insertion. These access maps, individually or in accord, provide an intuitive visualization of the region of intervention. The generation of these maps is described in more details in the follow-up paragraphs.

Direct Impact Map: The first map in our path-planning approach generates the projection of vital brain structures. The vertices on the skin surface whose path trajectory passes directly through the vital tissue should be considered unsafe and discarded. We start by considering all the vertices as safe incision points, thus initializing $\mathbf{V}_{\text{safe}} = \mathbf{V}$. Vital tissues are represented in form of a triangular mesh $\mathbf{M}_v = (\mathbf{V}_v, \mathbf{F}_v)$, with \mathbf{V}_v vertices and \mathbf{F}_v faces. A line segment is drawn from the target point \mathbf{t} to each vertex \mathbf{v} , where $\mathbf{v} \in \mathbf{V}_s$. If the line segment intersects any triangular face \mathbf{f} , where $\mathbf{f} \in \mathbf{F}_v$, the corresponding vertex is treated unsafe and removed from \mathbf{V}_{safe} . Thus, at the end of this step \mathbf{V}_{safe} consists of only those vertices, which guarantees that the path drawn from them never hits the vital tissue.

Proximity Map: The above direct impact map ensures that the trajectory of the pre-planned path will not intersect the vital tissue. There are situations

when the direct impact map may not be sufficient and additional information or processing may be needed. One such situation is when for a particular path the interventional tool passes very close to a region of the vital tissue without directly impacting it. In such a case, even a minute deviation from the pre-planned path could result in a serious damage to the vital tissue. Another challenge is that the different interventional tools have different diameters or thickness. The direct impact map does not take into account the thickness of the tool; thereby only using the direct impact map may bring the tool to very close proximity and even puncture the vital tissue. To address this issue, we incorporate a safe 3D buffer region that encloses the vital structures.

For every vertex $\mathbf{v} \in \mathbf{V}_{\text{safe}}$ on the skin surface, we try to compute the proximity for the vertex as:

$$PR(\mathbf{v}) = \arg \min_{e_{ij} \in E_v} (f_{v,t}(v_i, v_j)) \quad (1)$$

where \mathbf{E}_v correspond to set of edges of the mesh \mathbf{M}_v . \mathbf{e}_{ij} is the edge between vertices $\mathbf{v}_i \in \mathbf{V}_v$ and $\mathbf{v}_j \in \mathbf{V}_v$. If there exist a line which intersects and is orthogonal to the line segments with end points $\langle \mathbf{v}_i, \mathbf{v}_j \rangle$ and $\langle \mathbf{v}, \mathbf{t} \rangle$, function $f_{v,t}()$ returns the minimum distance between these two line segments. Otherwise we check, if there exists any orthogonal projection from vertex \mathbf{v}_i or \mathbf{v}_j on the trajectory of the path defined by the line segment with end points \mathbf{v} and \mathbf{t} , function $f_{v,t}()$ returns $\min(d_i, d_j)$ where d_i or d_j is the shortest distance of the vertex \mathbf{v}_i or \mathbf{v}_j from the line segment.

For a path with the starting point at vertex \mathbf{v} , $PR(\mathbf{v})$ is the minimum distance between the vital tissue and the line segment representing the trajectory of the insertion path. It ensures that if any insertion is made through vertex \mathbf{v} there will not be any vital structure at least at a distance $PR(\mathbf{v})$ from the insertion path. Thus, a safe buffer region can be created around the vital structures by removing those vertices from the set \mathbf{V}_{safe} whose $PR(\mathbf{v})$ falls below a given threshold PR_T .

The same concept is used for considering the thickness of surgical instruments. If we consider a cylinder with radius equal to $PR(\mathbf{v})$ and central axis aligned along the path trajectory starting from vertex \mathbf{v} to target \mathbf{t} , there won't be any vital structure in the vicinity of the cylinder. Thus, it is safe to insert a surgical instrument at \mathbf{v} whose thickness is less than $PR(\mathbf{v})$.

Path Length Map: The above two maps ensure that the interventional tool maintains a minimum distance $PR(\mathbf{v})$ from the vital structures. An additional concern in an intervention might be the depth of traversed tissue; in general, the shorter the distance, the less the risk of trauma even to non-vital structures. Therefore, we introduce a third map that shows the traversed length from the target to the skin. This map is generated by calculating the path length $PL(\mathbf{v})$, of the target from each vertex $\mathbf{v} \in \mathbf{V}_{\text{safe}}$. Those vertices are excluded from \mathbf{V}_{safe} for whom the value of $PL(\mathbf{v})$ is greater than a given threshold PL_T .

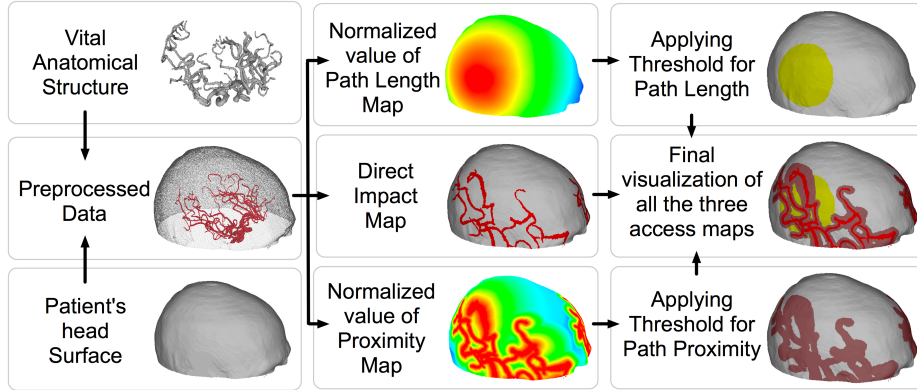


Fig. 1. Illustrates the generation of the access maps. In case of ‘Normalized value of Proximity Map’ the red color corresponds to insertion points whose access path is closer to the vital structure. In ‘Normalized value of Path Length Map’ red color corresponds to shorter distances of the target from the surface.

The process of generating the above access maps is schematically illustrated in Fig. 1. For the sake of a clear explanation, we assign blood vessels as one of the vital anatomical structures. The preprocessed data consist of the patient’s head surface, blood vessels and the target point registered together. The steps involved in data preprocessing are explained in details in section 2.2. A suitable set of insertion points \mathbf{V}_{safe} can be found on the patient’s head for a given neurosurgical interventional procedure by setting the values of the two thresholds PR_T and PL_T for the normalized value of the proximity map and the path length map, respectively. The final set of insertion points is given as:

$$\begin{aligned} \mathbf{V}_{\text{safe}} = & \{ \mathbf{v} | \mathbf{v} \in \mathbf{V}_s \} \\ & - \{ \mathbf{v} \in \mathbf{V}_s \text{ which directly intersect vessels} \} \\ & - \{ \mathbf{v} | \mathbf{v} \in \mathbf{V}_s, PR(\mathbf{v}) < PR_T \} \\ & - \{ \mathbf{v} | \mathbf{v} \in \mathbf{V}_s, PL(\mathbf{v}) > PL_T \} \end{aligned}$$

2.2 Data Preprocessing

We tested this approach using MRI data. A high resolution T2 weighted 3D spin-echo multislice set and a time-of-ight (TOF) MRA of the same subject was used for extracting the surface of the head and the brain vasculature, respectively. The extracted brain vasculature is assigned as the vital tissue in this work.

The multi-contrast MR data were subjected to a three-step pre-processing to be used in the planning and visualization algorithms. The first step entails segmentation of the MRA and T2-weighted images. Specifically, to segment the blood vessels from the MRA, we used a region-oriented segmentation techniques

of thresholding and region growing [1]. In the original TOF images, the vessels appear brighter relative to the surrounding tissue. First, we applied thresholding and then a connectivity filter based on region growing by selecting the base of the vessel as the seed point. Subsequently, the outer surface of the head was extracted from the T2-weighted MR images by applying a threshold to segment the region outside the head (like a negative mold) and then applying an inversion filter to get the inside region. Segmentation of the head surface stopped just above the nose and ears. In the second step, we used the marching cube algorithm [3] to construct 3D iso-surfaces that surround the high intensity pixels of the segmented images (e.g. vessels from the MRA). The resulting 3D model of the skin and the vessels is represented in form of a triangular mesh. Since the mesh generated by the marching cube algorithm also includes noise in the form of surface artifacts, we first applied the Laplace+HC mesh smoothing algorithm [4] followed by a low pass filter [2]. To avoid possible excess smoothing that may cause shrinkage of the mesh, the number of iteration steps for both algorithms was carefully chosen to ensure no or minimal volume shrinkage. The final step involves the co-registration of the two 3D models. This was straightforward in our studies, since we used the inherent coordinate system of the MR scanner that is shared among all the image sets and there was no patient's head motion during MR scans. At the end of the pre-processing step, we had two 3D models of the angiograms from the MRA and the skin surface from the T2-weighted images. The data-preprocessing step may lead to formation of mesh with non uniform sample density of triangles. In such a case, isotropic remeshing algorithms could be used. Secondly, to ensure fine-scale discretization of the head surface, the resultant mesh could be further subdivided as per the requirement of the interventional procedure. Those data along with the target point were then used as input to the path planning approach detailed in section 2.1.

3 Results

This proposed method was applied to test cases representing a wide range of target morphologies, i.e. the positions of the target points were selected as per the requirements of given surgical procedures. Below we describe and discuss two specific cases to illustrate its performance for different proximities of the target relative to a vital anatomy (e.g., blood vessel).

Test Case 1: In the first case, the target was positioned in the cerebrum region of the brain. A maximum threshold of 40.26 mm for path length and minimum threshold of 4.00 mm for the distance from blood vessels were specified. The minimum value of the path length from the head surface to the target point is 37.21mm. Three insertion points namely IP1, IP2, IP3 were selected (as shown in Figure 2) on the outer surface of the head. Among all the insertion points, point IP1 is the closest to the target from the surface at a distance 37.99 mm. Although an insertion made through that point would have shorter path length, the path of insertion of the interventional tool passes directly through the blood vessel. Therefore a path might be shorter but not safe. The insertion path from Point

IP2 (positioned at the boundary of the proximity map) to the target although being at the safe distance of 4.00 mm, the interventional tool need to travel a long distance of 59.64 mm. For the given threshold value, IP3 is the optimal point with a minimum distance of 4.74 mm from the insertion path and a path length of 39.67 mm.

Test Case 2: In the second test case, the target was positioned very close to the vessel. Path length threshold is set to a value of 34.93mm. Threshold for a minimum distance of the insertion path from the vessel is set to 1.48 mm. The minimum value of the path length from the head surface to the target point is 34.37 mm. In the right of figure 2, the blood vessel that is very close to the target, has a broader proximity map, compared to other blood vessels. In spite of the vessel being very close to the target, the buffer region ensures that the interventional tool maintains a minimum distance from the vessel and is still able to hit the target. In this test case, IP1 is the optimal insertion point.

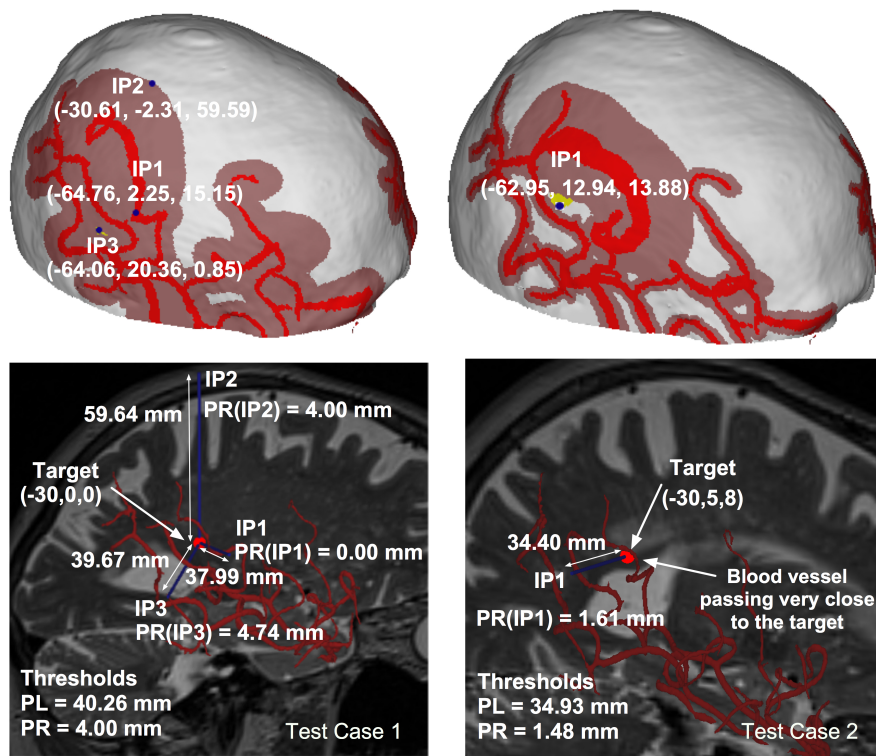


Fig. 2. Test Cases: test case 1 (left) and test case 2 (right). Top figures shows 3D model of patient's head illuminated with access maps and selected insertion points. The bottom figure shows the morphology of the area relative to MR images.

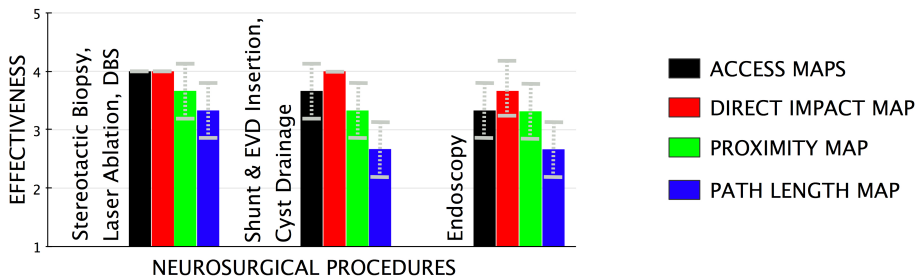


Fig. 3. Shows the effectiveness of the access maps (in conjunction as well as individual) for different neurosurgical interventional procedure.

Preliminary Evaluation: To evaluate the effectiveness of our approach, we performed a preliminary evaluation by collecting feedback from neurosurgeons. As suggested by Brunenberg et al. [6], we also invited three neurosurgeons for our preliminary evaluation. The three neurosurgeons were asked to rate the effectiveness of the access maps for different neurosurgical interventional procedures on a scale of 1 to 5 where 1 stands for ‘not very effective’ and 5 for ‘extremely effective’. Figure 3 shows the means and the standard deviations of the effectiveness in the form of a bar graph. The results (in figure 3) show that neurosurgical procedures such as stereotactic biopsy, laser ablation of tumors, and deep brain stimulation (DBS) could be planned more effectively with the help of our access maps. Also, the given approach is relatively easy to be used by a neurosurgeon in an interventional suite as it only requires tuning the two parameters (PR_T and PL_T) for a given vital structure as per the neurosurgical procedure.

In all neurosurgical procedures, the path length map may not be as effective as other access maps. This mainly due to the following two reasons. First, the path length can be adequately determined manually during preoperative planning. Second, it is not necessary that the path traversed by an intervention tool should be the shortest. In case of the endoscopic procedure, the target is usually large (comparing to the single point used in the approach) and the entry points are standardized. Therefore, image guidance is not as helpful as that in other stereotactic procedures. As a result, the access maps tend to be ineffective in planning these kinds of procedures.

Most of the neurosurgical interventions are planned by analyzing the 3D data of brain images in sagittal, coronal and transverse planes. The neurosurgeon finalizes the path by inspecting the image slices perpendicular to the bird’s-eye view along the insertion path and looking for any abnormalities. Image guidance systems (such as from BrainLab and Radionics) are used for the purpose of preoperative planning. The survey also included questions regarding the integration of the proposed approach with existing systems. If the proposed visualization technique is used in conjunction with the existing systems, it would provide improvement in terms of time required for trajectory planning as it has the potential to make the process less fiddly. However, the access maps do not provide

any improvements in terms of accuracy or precision of how the interventional tool would follow the pre-planned path. The accuracy solely depends upon the kind of stereotactic frame system used during the time of intervention.

4 Discussion

In the current test cases, we limited the vital tissue to blood vessels only. Although blood vessels are vital structures, other important anatomical structures need to be considered, depending on specific neurosurgical procedures and the targeted areas. Considering other soft tissues and neuronal pathways would further improve the work. The work of [14,16] shows the use of brain atlases for path calculation. Incorporating information derived from different atlases and surgeon experience level [15] would help in better risk assessment. We plan to expand this work by incorporating data from other modalities including functional Magnetic Resonance Imaging (fMRI) and Diffusion Tensor Imaging (DTI) and thus extend our classification component depicting the neural and metabolic activities of the brain. However, as this is a feasibility study, this limitation does not affect the generality of our method. Another limitation of the current work is the inclusion of only healthy volunteers, and as a consequence, we used virtual targeted tissues and artificial thresholds. In the future we will expand the work to include cases of patients.

The current work assumes that the brain tissue is rigid; we did not consider any possible tissue shifting when the patient is transferred from the imaging to the surgical suite, or to the procedure (i.e. intra-operative changes). As it may be appreciated, even a slight shift of a deeply seated brain structure during the incision or the advancement of the interventional tool may result in the damage of the vital tissue or missing the target. Apart from brain shift, registration errors could occur. The possible reasons of the registration errors could be either slipping of the fiducial markers or the displacement caused by patients' baggy skin. Some of the neurosurgical needles tend to bent as they penetrate into the tissue layer. In the future, we plan to expand and investigate appropriate safety margins to account for such deformations.

5 Conclusion

In this work, we present a method for visualizing and planning a neurosurgical intervention with straight access. The basic concept of our approach is the generation of various access maps on the surface of the skin of the patient's head. These access maps can guide a neurosurgeon in selecting an entrance point for accessing a specific targeted anatomical structure inside brain. The basis for generating these maps is the classification of tissue from images of different contrast suitable for tissue identification, segmentation and eventual classification. With the help of the direct impact map, impingement of the interventional tool on a vital anatomical structure can be avoided. Subsequently, with the help of the proximity map, the trajectory of a straight line of access from the incision

point to the target can maintain a minimum distance from the vital structures, thereby creates a safe buffer region.

While this method was implemented using brain MRI and neurosurgical interventional paradigms, it might be applicable to other anatomical areas and other imaging modalities. Our preliminary user study results showed that our approach is effective and visually intuitive for neurosurgeons. Moreover, the concept of projecting vital information on the surface of the skin was proved efficient for alleviating the challenge associated with the visualization, understanding and manipulation of 3D medical data sets. Such kind of visualization is a critical factor in the interventional suite to reduce the workload and increase accuracy.

Acknowledgments This work was supported in part by NSF CNS-0932272, NSF IIS-0914965, and Texas NHARP 003652-0058-2007. Any opinions, findings, and conclusions or recommendations expressed in this material are those of the authors and do not necessarily reflect the views of the funding agencies.

References

1. Luo, S., Zhao, Y.: Extraction of Brain Vessels from Magnetic Resonance Angiographic Images: Concise Literature Review, Challenges, and Proposals. In: Proc. of IEEE EMBS, 1422-1425 (2005)
2. Taubin, G.: A signal processing approach to fair surface design. In: Proc. of SIGGRAPH'95, 351-358 (1995)
3. Lorensen, W.E., Cline, H.E.: Marching Cubes: A High Resolution 3D Surface Construction Algorithm. In: Proc. of SIGGRAPH'87, 163-169 (1987)
4. Vollmer, J., Mencl, R., Mller, H.: Improved Laplacian Smoothing of Noisy Surface Meshes. In: Proc. of Eurographics'99, 131-138 (1999)
5. Nowinski, W.L.: Virtual Reality in Brain Intervention. In: IEEE Symp. on Bioinformatics and Bioengineering, 245-248 (2004)
6. Brunenberg, E.J.L., Bartroli, A.V., Vandewalle, V.V., Temel, Y., Ackermans, L., Platel, B., Romenij, B.M.H.: Automatic Trajectory Planning for Deep Brain Stimulation: A Feasibility Study. In: MICCAI, 584-592 (2007)
7. Lee, J.D., Huang, C.H., Lee, S.T.: Improving stereotactic surgery using 3-D reconstruction. IEEE Eng. in Med. and Bio. Mag., vol. 21, 109-116 (2002)
8. Bourbakis, N.G., Awad, M.: A 3-D visualization method for image-guided brain surgery. IEEE Trans. on Systems, Man, Cybernetics, vol. 33, 766-781 (2003)
9. Fujii, T., Emoto, H., Sugou, N., Mito, T. Shibata, I.: Neuropath planner-automatic path searching for neurosurgery. In: Proc. of Computer Assisted Radiology and Surgery (CARS), vol. 1256, 587-583 (2003)
10. Beyer, J., Hadwiger, M., Wolsberger, S., Buhler, K.: High-Quality Multimodal Volume Rendering for Preoperative Planning of Neurosurgical Interventions. IEEE Trans. on Vis. and Comp. Graph., vol. 13, 1696-1703 (2007)
11. Joshi, A., Scheinost, D., Vives, K.P., Spencer, D.D., Staib, L.H., Papademetris, X. Novel interaction techniques for neurosurgical planning and stereotactic navigation, IEEE Trans. on Vis. and Comp. Graph., vol. 14, 1587-1594 (2008)
12. Seigneuret, J.F., Jannin, P., Fleig, O.J., Seigneuret, E., Mor, X., Raimbault, M., Cedex, R.: Multimodal and Multi-Informational Neuronavigation. In: CARS - Computer Assisted Radiology and Surgery, 167-172 (2000)

13. Serra, L., Kockro, R.A., Guan, C.G., Hern, N., Lee, E.C.K., Lee, Y.H., Chan, C., Nowinski, W.L.: Multimodal Volume-based Tumor Neurosurgery Planning in the Virtual Workbench. In: MICCAI'98, 1007-1015 (1998)
14. Vaillant, M., Davatzikos, C., Taylor, R. H., Bryan, R. N.: A path-planning algorithm for image-guided neurosurgery. In Proc. of Computer Vision, Virtual Reality and Robotics in Medicine and Medical Robotics and Computer-Assisted Surgery, 467-476 (1997)
15. Tirelli, P., De Momi, E., Borghese, N. A., and Ferrigno, G.: An intelligent atlas-based planning system for keyhole neurosurgery. Int'l J. of Computer Assisted Radiology and Surgery (JCARS), vol. 4, 85-89 (2009)
16. Popovic, A., and Trovato, K.: Path planning for reducing tissue damage in minimally invasive brain access. In Computer Assisted Radiology and Surgery (CARS 2009), supplemental S132-S133, (2009)